ACS APPLIED MATERIALS & INTERFACES

www.acsami.org Research Article

Functionality of Surface Mycelium Interfaces in Wood Bonding

Wenjing Sun, Mehdi Tajvidi,* Caitlin Howell, and Christopher G. Hunt

Cite This: *ACS Appl. Mater. Interfaces* 2020, 12, 57431−57440 Read Online

ACCESS | Metrics & More | Article Recommendations

ABSTRACT: Filamentous fungi have been considered as candidates to replace petroleum-based adhesives and plastics in novel composite material production, particularly those containing lignocellulosic materials. However, the nature of the role of surface mycelium in the adhesion between lignocellulosic composite components is not well-known. The current study investigated the functionality of surface mycelium for wood bonding by incubating *Trametes versicolor* on yellow birch veneers and compared the lap-shear strengths after hot-pressing to evaluate if the presence of surface mycelium can improve the interface between two wood layers and consequently improve bonding. We found that the lap-shear strength of the samples was enhanced by the increase of surface mycelium coverage up to 8 days of incubation (up to 1.74 MPa) without a significant wood weight loss. We provide evidence that the bottom surface of the mycelium layer is more hydrophilic, contains more small-scale filamentous structure and contains more functional groups, resulting in better bonding with wood than the top surface. These observations confirm and highlight the functionality of the surface mycelium layer for wood bonding and provide useful information for future developments in fully biobased composites manufacturing.

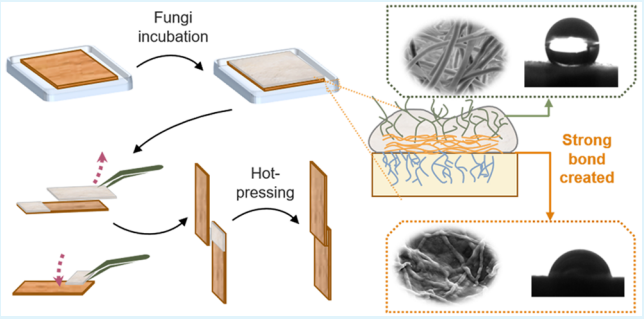

KEYWORDS: *mycelium, bonding, lap-shear strength, wood, interface, veneer*

INTRODUCTION

Mycelium biocomposites are novel materials that provide the opportunity to achieve a biobased circular economy, and mycelium has become a popular novel biomaterial for multiple applications, including textile, packaging, construction, and other applications.[1,2] By inoculating filamentous white-rot fungi in particles of agricultural and other lignocellulosic materials for days and drying afterward, a foam-like structure of mycelium-bonded composite with a density range of 0.06−0.30 g cm^{-3} can be produced.[3] Composite panels with a higher density could be further generated by adding heat and pressure to those mycelium foams. These kinds of panels have components and structures similar to the traditional lignocellulosic-based particleboards and are being investigated as a potential replacement for formaldehyde-based adhesive-bonded panels.[4−6] Opportunities also exist for applications in low-density packaging and insulation products. Multiple biobased adhesives have been explored and developed in the lignocellulosic biocomposites manufacturing in the past few decades in response to the increasing environmental awareness. Proteins, carbohydrates, lignin, tannin, and other natural biopolymers have all been investigated as wood adhesives. Some of these adhesives even have had commercial success.[7] However, the adhesives market is large, with many products and needs, leaving opportunities for a variety of approaches. Hot-pressed mycelium-lignocellulosic biocomposites are an alternative path to 100% biobased, eco-friendly biocomposites.

The bonding mechanism of a hot-pressed mycelium biocomposite is not yet well understood. The major components of traditional biocomposites, lignocellulosic materials, have been used to produce binder-less boards using a similar procedure, which functions mainly by softening and plasticizing wood, potentially aided by reactions stemming from hemicelluloses and lignin.[8,9] Fungal pretreatment may accelerate this effect by degrading the polymers into smaller molecules.[10−13] At the initial stage of colonization, white-rot fungi secrete enzymes that create lignin oxidants.[14,15] The released lignin radicals could potentially contribute to covalent bonding.[16] Several studies have suggested positive correlations between the enzyme loading and the strength of the resulting composite.[17−19]

The mycelium body, which works as an entanglement in foam-like mycelium composites, may also contribute to the bonding. During the colonization of fungi on lignocellulosic

Received: October 9, 2020
Accepted: December 1, 2020
Published: December 11, 2020

https://dx.doi.org/10.1021/acsami.0c18165
ACS Appl. Mater. Interfaces 2020, 12, 57431−57440

substrates, hyphae first develop and elongate on the substrate surface from originally loaded mycelial fragments.[20,21] This layer of aerial hyphae or surface mycelium significantly changes the surface morphology and surface energy of the substrate.[22−24] At the same time, the outer layer of fungal hyphae contains proteins and glycoproteins,[25,26] which are typical adhesive candidates and may act as adhesive in the composite system.[27]

Because of the complexity of such systems, very limited evidence has been provided on the details of the role of surface mycelium on bonding in lignocellulosic biocomposites. The solid substrates are usually in small geometries (particles or fibers), and therefore, it is hard to separate the surface mycelium from them, leading to problems in decoupling of the effects of multiple variables. For the same reason, we have not found any reported research on developing pure fungal mycelium as a stand-alone adhesive.

In this article, we specifically investigated the wood bonding ability of fungal mycelia and components that might be contributing or detracting from bond strength. We made the first attempt at quantifying the adhesive strength of a pure surface mycelium layer through a unique growing system. By controlled growth of fungi on veneer, the surface mycelium could be easily separated. Using this system, we incubated white-rot fungi *Trametes versicolor* on yellow birch veneers for different time periods. The growth behavior of surface mycelium, the change of surface properties of veneers, and their influence on bonding strength were investigated in light of the contributions of various interfaces. The difference between the top and bottom surfaces of the mycelium layer was also discovered and compared.

EXPERIMENTAL SECTION

Materials. Yellow birch (*Betula alleghaniensis* Britt.) wood veneers with a thickness of 0.61 (±0.04) mm were kindly supplied by Columbia Forest Products LLC (Presque Isle, ME). *Trametes versicolor* was supplied by Ecovative Design LLC (Green Island, NY) and had been maintained on agar plates at 4 °C and was preincubated on malt extract agar (MEA) plates before the incubation process. Weldwood carpenter's wood glue (DAP Products Inc. Baltimore, MD) was purchased and used for the lap-shear experiment.

Mycelium Incubation. The incubation methods were modified from the literature.[28,29] Yellow birch veneer samples with the dimensions of 80 mm (length) × 80 mm (width) were steam sterilized at 121 °C for 60 min and soaked for about five seconds in 2% (w/v) corn steep liquor (CSL) (Sigma-Aldrich, Saint Louis, MO) containing suspended fungal mycelium. One MEA plate overgrown by the fungus was mixed in 150 mL of 2% (w/v) sterile CSL in a tissue grinder before they were transferred to Petri dishes containing MEA. Plastic canvas meshes were used as supports in between the veneer and agar. The Petri dishes were incubated at 28 °C, 80% relative humidity (RH) for up to 20 days.

Weight Loss of Wood Veneers and Weight Gain of Surface Fungal Mycelium. After different incubation periods, the surface mycelium was separated from the veneers. For earlier growth days, the mycelium was removed by using a stainless-steel ruler pushing to the side. At later stages of incubation and after the mycelium formed a mat, it was carefully peeled off with tweezers. Both the veneer and the surface mycelium layer were dried in a sequence of elevated temperatures (40 °C, 24 h; 60 °C, 24 h; 103 °C, 24 h). The weight loss of wood veneers was calculated by the change of dry weight before and after incubation. The weight gain of fungal surface mycelium was the direct dry weight of the obtained surface mycelium from a full piece of veneer (80 mm × 80 mm). Weight loss/gain of five replicates were calculated for each group.

Stereomicroscopy. Bright-field images were captured using a Nikon Ni-E (Nikon Instruments Inc., Melville, NY) stereomicroscope with Nikon Plan Fluor 10× PH1 DL 0.3 NA and 40× PH2 DLL 0.75 NA. Z-stack images were acquired at 10 μm intervals from the first hyphae to 200 μm and processed using the Extended Depth of Field (EDF) plugin in the image analysis software Fiji (ImageJ 1.52p, National Institutes of Health).[30]

Hot-Press and Lap-Shear Samples Preparation. The process of hot-press and lap-shear samples preparation is shown in Figure 1.

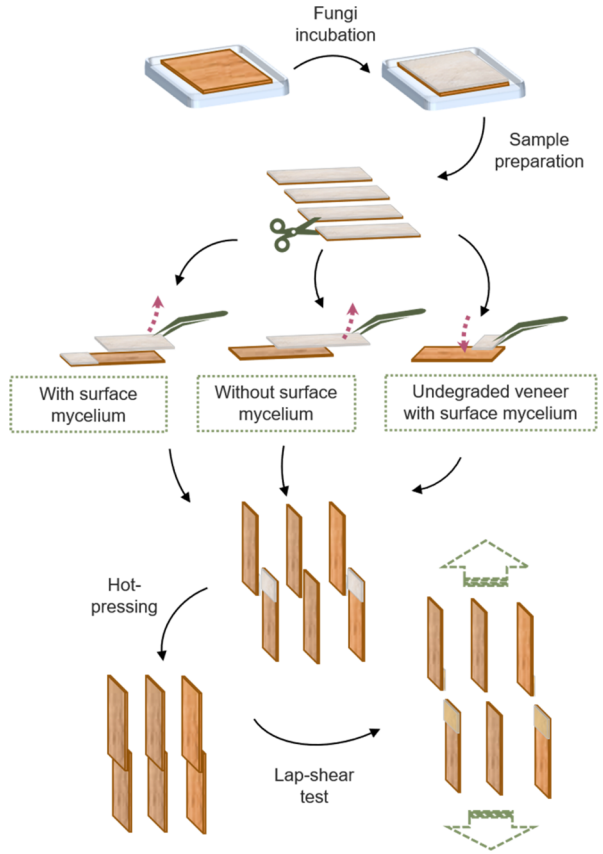

Figure 1. Schematic presentation of the procedure of hot-pressing and lap-shear sample preparation.

After incubation, the wood veneers were cut into strips of 80 mm × 20 mm before hot-pressing. The surface mycelium was either entirely removed or maintained in the lapping area (20 mm × 20 mm) for comparison. All lap-shear samples were hot pressed at 180 °C for 5 min. The pressure was controlled at 2.78 MPa. A slight densification of wood veneers under this pressure could be expected, but this was the lowest manageable pressure to apply using our hot press and it was kept constant for all experiments.

To exclude the change in wood surface and to compare the top and bottom position differences of the surface mycelium layer, a group of surface mycelium-bonded untreated veneers were also prepared. The removed mycelium layers were put in between two undegraded wood strips in different configurations (as depicted in Figure 1) and hot pressed under the same conditions. Untreated autoclaved wood specimens and commercial wood glue (spread rate: 30 mg per glue-line) bonded specimens were also prepared for comparison. To minimize the influences from other processing steps, the undegraded veneers were also autoclaved and saturated by water for 24 h before hot-pressing.

Lap-Shear Strength Test. The lap-shear tests were carried out on an Instron 5966 (Instron, Norwood, MA) with a 10 kN capacity load cell. The hot-pressed samples were conditioned at 23 ± 2 °C and 50 ± 2% RH for 48 h (adequate to reach a constant mass). The crosshead speed was 0.5 mm/min, and the initial gauge length was 40

https://dx.doi.org/10.1021/acsami.0c18165
ACS Appl. Mater. Interfaces 2020, 12, 57431−57440

mm. Twelve replicates were tested for each group. Wet strength tests were carried out by soaking bonded specimens in distilled water at room temperature 20 ± 1 °C for 48 h and testing immediately.

Scanning Electron Microscopy (SEM). The microstructures of the lap area of the samples and the top and bottom surfaces of the mycelium layer were analyzed using an Amray 1820 scanning electron microscope (SEM) (Amray Inc., New Bedford, MA) at an accelerating voltage of 10 kV. The samples were placed on specimen mounts with double-sided carbon tape and ground on all edges with conductive silver paint and sputter coated with 3 nm of gold−palladium.

Thermogravimetric Analysis (TGA). Thermal stability evaluation was carried out under nitrogen gas on a TGA Q500 (TA Instruments, New Castle, DE) with a high-resolution (Hi-Res) option from room temperature to 600 °C. In the Hi-Res approach, the heating rate is dynamically and continuously modified, ranging from 0.001 °C min^{-1} to the maximum heating rate (20 °C min^{-1}) in response to changes in the decomposition rate of the sample. The resolution and sensitivity settings were 4.0 and 1.0 °C, respectively. The TGA results are shown as the variation of the sample mass (TG) and as a derivative weight loss (DTG) curve corresponding to the temperature.

Attenuated Total Reflection-Fourier Transform IR (ATR-FTIR). ATR-FTIR spectra of the surfaces were obtained using a Spectrum Two IR spectrometer (PerkinElmer, Waltham, MA). All spectra were obtained in the range 4000−600 cm^{-1} with a 4 cm^{-1} resolution, accumulating 32 scans. The tested samples were all in room condition. To ensure the reproducibility of the obtained spectra, three replicate specimens were measured.

Water Contact Angle Analysis. The contact angle analysis was carried out using a mobile contact angle analyzer (KRUSS GmbH, MSA, Hamburg, Germany) and the corresponding software for this device. For each measurement, one 1 μL drop of water was applied on a random area of the surface. The measurements were made on the same mycelium and wood samples used in the weight change testing. Six measurements were carried out per sample 2 s after the drop touched the surface.

Statistical Analysis. The obtained lap-shear strength values were analyzed using one-way analysis of variance (ANOVA) to determine statistical differences between the means. A Tukey's honestly significant difference (HSD) multiple comparison test was then performed to further assess the significance level of the mean values for each treatment level. All comparisons were made at a 95% confidence level. All the analyses were performed using RStudio (Version 1.2.5033).

RESULTS AND DISCUSSION

Growth Behavior of Mycelium on Wood Surface. The development of aerial hyphae on the veneer surface is shown in the photos in Figure 2A,B and the microscopic images presented in Figure 3. Ground mycelial fragments were mixed with nutrients and dispersed on the surface of veneers on Day 0. There was no visible colonization on Day 0 and Day 2. The aerial hyphae started to be visible on Day 4. However, they were not very easy to be seen vertically (Figure 2A) but were more visible when viewed at an angle (Figure 2B). The microcolonies continued to expand and approach one another, and on Day 8, they nearly covered the entire surface. After that, the aerial hyphae started to grow thicker and formed a packed aerial layer until Day 18. Figure 2C shows the weight percent loss of veneer and weight gain of surface mycelium after different incubation days. With the colonization of fungi, the weight of removable surface mycelium increased dramatically from Day 6 to Day 8 and continued until Day 12. There was no significant difference ($p > 0.05$) from Day 12 to Day 18 in the weight of the grown surface mycelium, which indicates that the degradation and the growth of mycelium were most likely

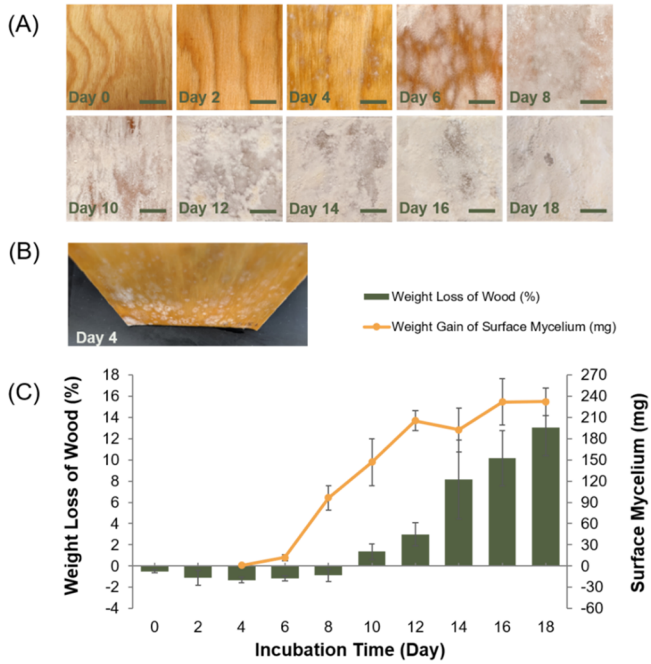

Figure 2. (A) Development of surface mycelium on yellow birch veneer over 18 growing days (scale bar: 2 cm). (B) Surface of Day 4 sample in a different viewing angle. (C) Weight loss of wood (%) and weight gain of surface hyphae (mg).

happening inside the wood substrate. On the contrary, there was no significant weight loss happening in wood veneers before Day 8. The negative percentages of weight loss come from the gained weight from the nutrient and mycelium (9.58 ± 2.38 mg on Day 0 and 21.44 ± 13.13 mg on Day 2, not shown in Figure 2). Starting from Day 6 until Day 18, there was a continuous wood weight loss, indicating the progressive degradation of wood substrate, corresponding well with the weight gain of the surface mycelium.

Stereomicroscopic images of the growth of surface mycelium on veneers after different incubation days are shown in Figure 3. Parts A, E, I, and M of Figure 3 depict the extended z-stack focus stacking images to better present the surface changes. Parts B−D, F−H, J−L, and N−P of Figure 3 reveal the images taken at different depths. Although ground mycelial fragments loaded on the veneer surface already existed on Day 0, they were almost not visible in the microscopy images (Figure 3A−D). On Day 4, the surface mycelium layer was still quite thin and the texture of the wood surface was still visible in the microscopic images (Figure 3E−H). When the surface mycelium layer was thick enough (Day 8 and Day 12), only branched hyphae could be captured in the applied depth.

Changes in Wood Surface and Thermal Properties. The colonization of the surface mycelium also remarkably altered the surface properties of the yellow birch veneer. Figure 4A shows an EDF microscopy image of a 20 day incubated veneer after the surface mycelium had been removed. It is obvious that there was almost no mycelium on the surface when comparing Figure 3E,I,M. After 4 days of incubation, the water contact angle increased from less than 100° to 125 ± 3° and then stayed relatively constant (no statistically significant change), as shown in Figure 4B. It is known that the outer layer of aerial hyphae contains a kind of hydrophobin protein that makes the mycelium surface hydrophobic[31,32] and helps fungi to escape from the aqueous environment and grow in air.

https://dx.doi.org/10.1021/acsami.0c18165
ACS Appl. Mater. Interfaces 2020, 12, 57431−57440

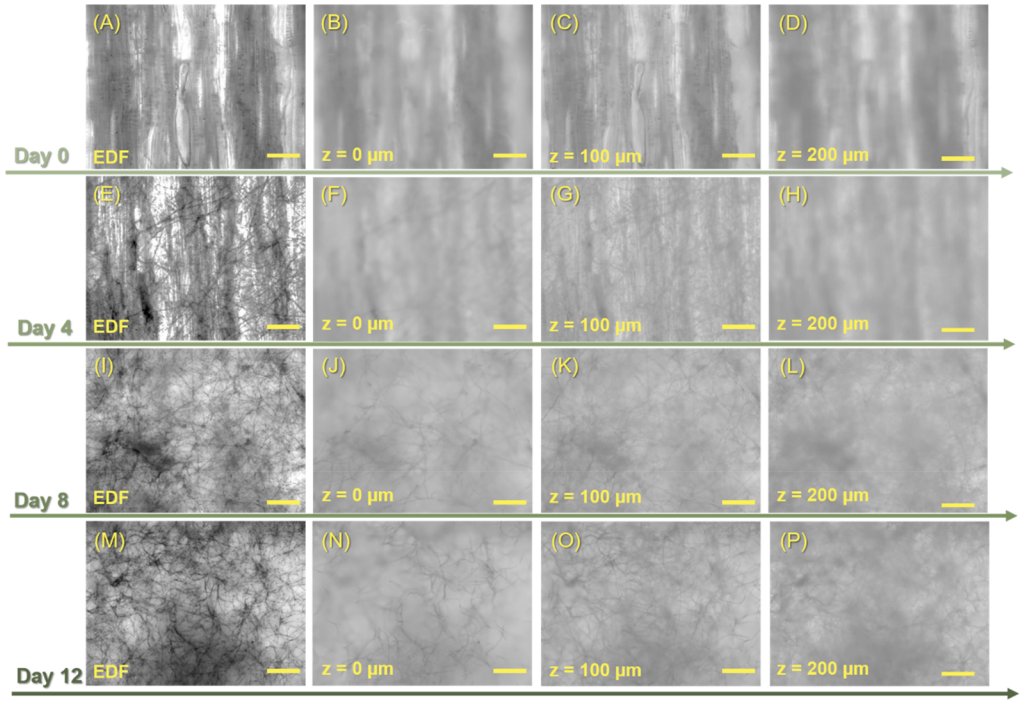

Figure 3. Stereomicroscopic images of the growth of surface mycelium on yellow birch veneers after different incubation days. (A, E, I, and M) Extended focus Z-stacking images. (B–D, F–H, J–L, and N–P) Images at different depths. Scale bar: 200 μm.

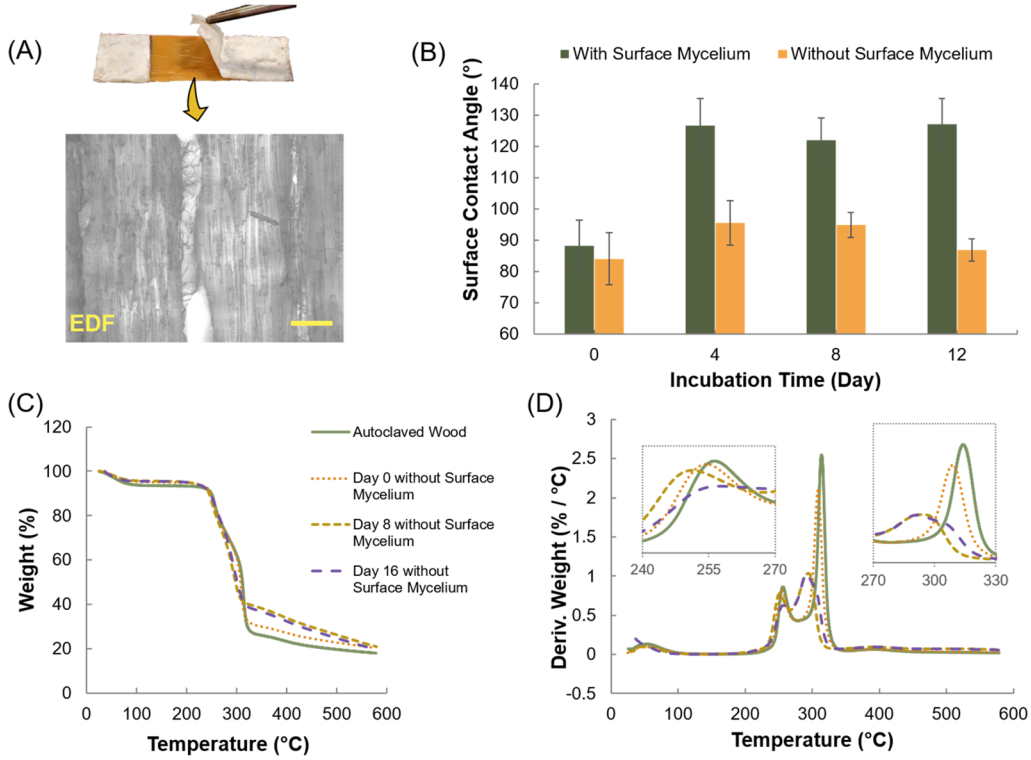

Figure 4. (A) Extended focus Z-stacking stereomicroscopic images of veneer surface after removing surface mycelium (Day 20), Scale bar = 200 μm. (B) Surface water contact angles of the veneers with and without surface mycelium after incubation. (C and D) TG (C) and DTG (D) curves of veneers without surface mycelium after incubation (Day 0 without surface mycelium indicates autoclaved wood immersed in ground agar and CSL mixture with no mycelial fragments).

Therefore, the initial increase in the water contact angle can be attributed to the coverage of the surface by aerial hyphae where the increased mass of mycelium at longer times does not affect wettability any further. On the surface after mycelium removal, the water contact angles dropped to 84°–95° and there was no significant difference ($p > 0.05$) among the different incubation times. We also compared the contact angle of undegraded wood veneers and autoclaved undegraded wood veneers (not

https://dx.doi.org/10.1021/acsami.0c18165
ACS Appl. Mater. Interfaces 2020, 12, 57431–57440

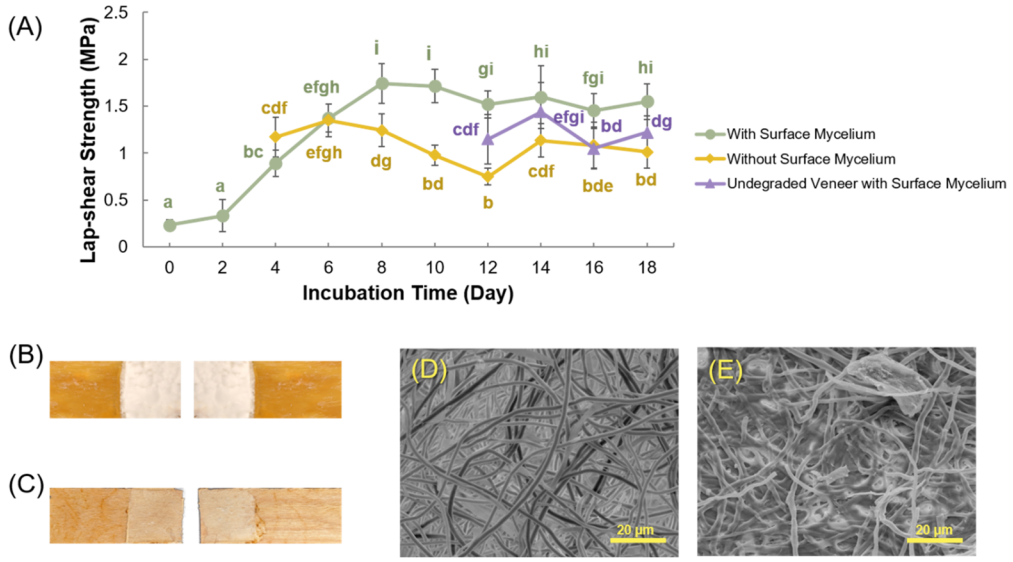

Figure 5. (A) Lap-shear strength of wood veneers after different incubation days with or without surface mycelium and undegraded wood with applied surface mycelium; data points with common letters are not significantly different at 95% confidence level ($p > 0.05$). (B and C) Lap area of "with surface mycelium" group before hot-pressing (B) and after the lap-shear test (C). (D and E) SEM images of the lap area of the "with surface mycelium" group before hot-pressing (D) and after the lap-shear test (E) (Scale bar: 20 μm).

shown) for reference. The contact angle of autoclaved veneer was 93 ± 11°, which was not significantly different ($p > 0.05$) from that of the degraded wood surfaces after removing the mycelium layer, indicating that fungal degradation did not have a significant effect on the surface wettability of wood. In contrast, the untreated wood veneer had a contact angle of 73 ± 10°, which was significantly lower than that of the autoclaved sample and corresponded well to the reported values in the literature.[33] An increased contact angle after autoclaving could possibly relate to the reorganization of the lignocellulosic polymeric components of wood surface due to the plasticization of lignin.[34]

Parts C and D of Figure 4 show the TG and DTG curves of the veneers without surface mycelium after different incubation days. For wood samples, the TG curve usually shows a three-step degradation: from start to around 220 °C as water and volatile extractives leave the sample; 220 to 360 °C as hemicelluloses, amorphous cellulose, and some lignin are mainly degraded; and 360 °C to the final temperature as lignin and cellulose degrade (Figure 4C).[35−37] When using a conventional fixed heating rate TGA, the degradation of hemicelluloses is usually shown as a left shoulder in the DTG curve, whereas the dynamic mode separated it as an individual peak (Figure 4D). As the fungi degraded wood components into smaller molecules, the thermal stability decreased correspondingly, which is shown in the DTG curves as the degradation peaks move to a lower temperature and also become broader along with the degradation time. The added nutrient also caused a similar trend when comparing the DTG curves of autoclaved wood and Day 0 wood but is not as extreme as in the case of the extended degradation days.

Bonding Properties. Figure 5A shows the lap-shear strengths of the three groups of veneers after various incubation times. The incubation times are different for the three groups with or without surface mycelium, because, before Day 12, a continuous mycelium mat was not fully produced or was too thin to be removed without damage. For the group of "with surface mycelium", the lap-shear strength generally showed a similar trend as that of the surface coverage of mycelium shown in Figure 2A. On Day 0 when there was only a small amount of nutrients and mycelium loaded on the wood surface, the lap-shear strength was as low as that of the bonded autoclaved undegraded wood (0.29 ± 0.09 vs 0.23 ± 0.06 MPa). The lap-shear strengths increased with the coverage of the mycelium on the surface. After the mycelium covered the whole surface, the increase of the mycelium mat thickness did not further improve bonding. The "without surface mycelium" group did not show a consistent trend, and the strength values generally remained stable with no statistically significant change regardless of apparent maximums and minimums. This observation might relate to the change in the wood components and functional groups at different degradation stages[17,38] or for some other unknown reasons. In practice, it is impossible to separate the surface mycelium from the small substrates of particles and fibers if the mycelium is grown on lignocellulosic particles or fibers, and therefore, a combination in which the mycelium body is present is more technically feasible. Although the details of this change are not in the scope of this paper, when comparing the "with" or "without mycelium" groups, it is evident that the additional growth of the surface mycelium layer had more contribution to bonding than the possible changes in the wood surface, as bonding undegraded wood with mycelium always gave equal or better results than bonding degraded wood without mycelium (Figure 5A). It could be concluded that both the surface mycelium and the change on the wood surface could promote bonding between wood surfaces, and the effect of surface mycelium is higher than the wood surface changes.

Microscopic images of the lap areas after failure provide more information regarding the failure modes. When looking at the lap area after the lap-shear test, the two groups that contained two layers of surface mycelium broke at the interface between the surface mycelia. This suggests that the adhesion between the two layers of surface mycelia is weaker than the adhesion between mycelium and wood. Compared with the images of the surface before hot-pressing (Figure 5B), the

https://dx.doi.org/10.1021/acsami.0c18165
ACS Appl. Mater. Interfaces 2020, 12, 57431−57440

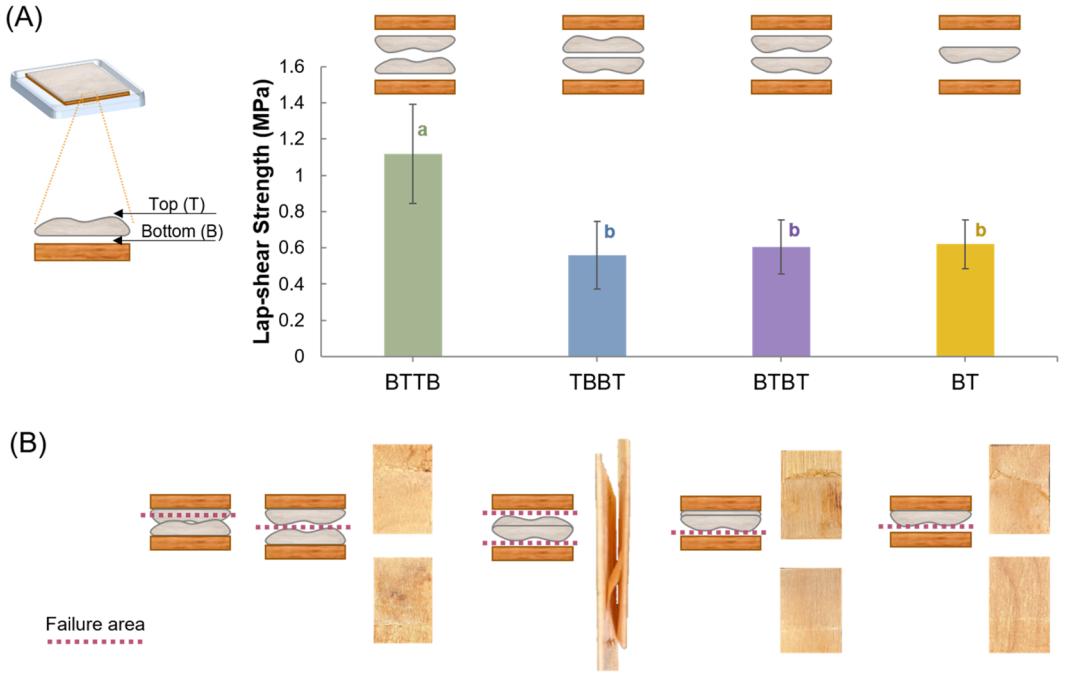

Figure 6. (A) Lap-shear strengths of the different surface contact of mycelium layers bonded undegraded veneers and the corresponding sketches; columns with common letters are not significantly different at 95% confidence level ($p > 0.05$). (B) Photos of the failure mode of each group and the corresponding sketches.

color of the mycelium layer changed from white to slightly transparent (Figure 5C), consistent with compression of the hyphal mat (Figure 5D,E). Underneath the flattened surface fibers, there was a much denser structure with more connected fibers and small holes, which probably originated from the bottom part of the surface mycelium layer or caused by compression.

Top vs Bottom Mycelium Surfaces. To understand the different factors influencing the bonding of the two mycelium surfaces, we arranged them in different lay-ups in terms of the surfaces contacting each other and repeated the same hot-pressing and lap-shear tests. As shown in Figure 6A, when growing on the surface of veneer, the mycelium surface that was exposed to air was termed the top surface (T), while the surface that was attached to wood was called the bottom surface (B). The mycelium layers were removed from the wood they grew on and were placed in between two undegraded veneers for lap-shear sample preparation. The four combinations are BTTB, TBBT, BTBT, and BT, respectively (Figure 6A). For the first three groups, two layers of the surface mycelium were used, while for BT, there was only one layer. The lap-shear strength of each group is shown in Figure 6A. The BTTB combination achieved the highest lap-shear strength of about 1.11 MPa, whereas the other three groups showed only about half of the strength (0.56−0.62 MPa). When looking at the failure modes shown in Figure 6B, the BTTB lay-up showed mycelium cohesive failure; TBBT, BTBT, and BT showed mycelium−wood adhesive failure, all from the top surface of the mycelium layer. On the basis of the failure modes, it can be concluded that the adhesion of the bottom surface of the mycelium layer is stronger than the top surface, both with wood and with mycelium itself. For the strongest BTTB group, it was hard to tell if the failure had happened in between the two top surfaces or within the matrix of mycelium body. In either case, it was stronger than the bond between the mycelium top surface and wood but weaker than the bond between the mycelium bottom and wood.

In view of the different behaviors of the top and bottom surfaces of the removed surface mycelium layer, further characterizations were performed to compare them in detail. As shown in the stereomicroscopic images in Figure 7A,B, both the top and bottom surfaces show entangled filamentous structures but at very different scales. The top surface is fluffier with less visible hyphae in the EDF light microscopy image (Figure 7A), whereas the bottom surface is quite dense (Figure 7B). In the higher magnification images taken by SEM, the individual hyphae on the top surface are distinguishable with a diameter of 2.0 ± 0.5 μm (Figure 7C). At the same time, the bottom surface shows a flat, sheet-like structure (Figure 7D). Under a higher magnification, individual hyphae could be identified within the sheet-like structure (Figure 7E). Similar hyphal fusion and pseudolaminar sheet formation of *T. versicolor* were reported in previous research.[39]

When comparing the FTIR curves of the top and bottom surfaces of the mycelium layer, there are also distinct differences, which we believe indicate differences in chemical composition. The spectra of the bottom surface show a higher peak in the region 3600−3000 cm^{-1}, which corresponds to the O—H and N—H stretching (Figure 7G). More differences are shown in the region between 1800 and 600 cm^{-1}. The two main peaks at around 1640 and 1545 cm^{-1} correspond to amide I (C═O stretch) and II (N—H bend and C—H stretch) vibrations in proteins,[40−42] which showed much higher intensities for the bottom surface compared with the top surface. This indicates that there were probably more proteins that existed on the bottom surface. Notably, the peak at 1540 cm^{-1} was almost invisible on the spectra of the top surface but that on the bottom surface was intense and broad and had a shoulder at about 1530 cm^{-1}. The region from 1470 to 1240 cm^{-1}, known as an amide III band, is complex and

https://dx.doi.org/10.1021/acsami.0c18165
ACS Appl. Mater. Interfaces 2020, 12, 57431−57440

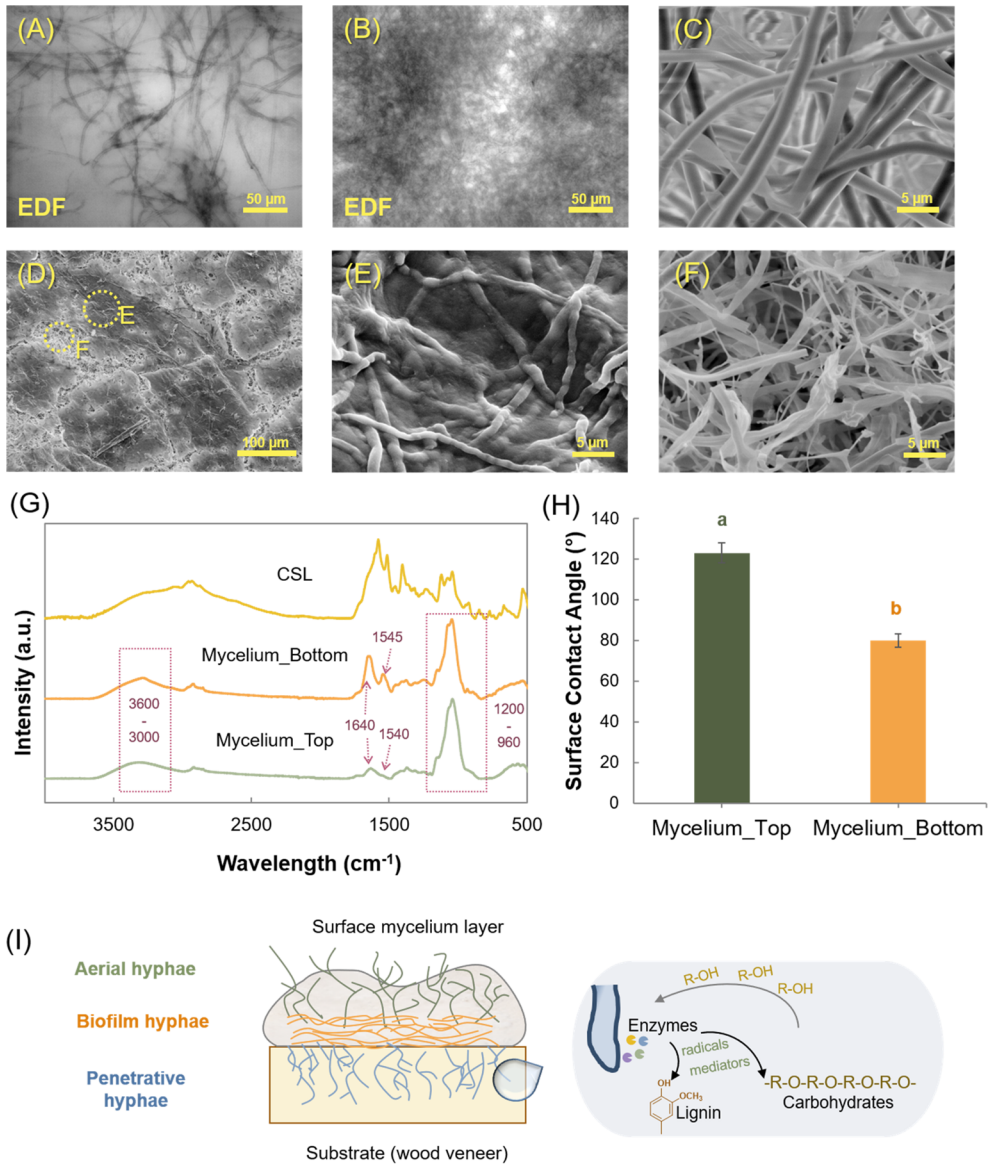

Figure 7. (A and B) Extended focus Z-stacking images of the top (A) and bottom (B) surfaces. (C−F) SEM images of the top (C) and bottom (D−F) surfaces. (G) ATR-FTIR spectra of CSL and top and bottom sides of surface mycelium. (H) Water contact angles of top and bottom sides of surface mycelium. (I) Schematic classification of hyphae and hyphal colonization of wood (gaining deep access through rays and branching through fibers).

affected by C—N from chitin and C—O from polysaccharides.[43] More peaks showed up in this region on the bottom surface than on the top surface, providing more evidence to the hypothesis that more protein exists on the bottom. The absorbance between 1200 and 960 cm^{-1} is attributed to polysaccharides in general.[43] The peak at 1073 cm^{-1}, probably due to the presence of O-substituted glucose residues,[44] is more intense in the spectra of the bottom surface, and the peaks at 970, 933, and 893 cm^{-1}, corresponding to C—C stretching in molecular backbone,[43] only showed up in the spectra of the bottom surface, indicating that there are also more varieties of sugars exposed.

It should also be mentioned that, as mycelium samples were dried directly without washing, the potentially remaining nutrition liquid (CSL) may also have contributed to the film-structure formation during the drying process. There are also some hyphae structures within the film structure, as shown in higher magnification in Figure 7F. Different from the hyphae from the top surface, there are more thread-like and tube-like structures on the bottom.[22] The FTIR spectra of CSL are also included in Figure 7G. CSL contains a large variety of nutrients and is enriched with carbon, nitrogen, and vitamins.[45,46] The FTIR spectra of CSL showed very different peaks compared with those of either the mycelium top or bottom surfaces. We believe that this evidence, and the general assumption that fungi consume CSL very quickly during colonization, means that IR spectra are not significantly affected by the CSL.

As shown in Figure 7H, the bottom surface of the mycelium layer was more significantly hydrophilic (contact angle 79 ± 3°) compared with the top surface (contact angle 123 ± 5°). This explains why the bottom surface that was attached to wood interacted better with wood surfaces, which also have relatively high surface energy.

According to Sugai-Guerios et al. in 2015, there are three basic types of hyphae in the solid-state fermentation system: the aerial hyphae, the biofilm hyphae, and the penetrative

https://dx.doi.org/10.1021/acsami.0c18165
ACS Appl. Mater. Interfaces 2020, 12, 57431−57440

hyphae, as shown in the sketch in Figure 7I.[20] As there were no hyphae visible on the wood surface after removing the surface mycelium layer (Figure 4A), the bottom mycelium layer must include the biofilm hyphae. Therefore, the top and bottom surfaces reveal the properties of aerial and biofilm hyphae, respectively. The biofilm hyphae hold more moisture and are shown as densely packed structures, whereas the aerial hyphae are directly in contact with the gas phase and hold air in their porous structure.[20] At the initial stages of white-rot fungal metabolism, enzymes are first released by the biofilm hyphae to the substrate through the diffusion medium, which is water. The enzymes secrete reactive oxygen species (ROS) and ROS precursors that react with wood components, and the degraded fragments such as monosaccharides are transported back to the hyphae through diffusion[47] (Figure 7I). Therefore, when removing the surface mycelium layer, the secreted proteins and the fragments of degraded substrate components can remain on the bottom surface and contribute to bonding through diffusion, hydrogen bonding, and potential covalent bonding after heat treatment. In addition, the surface itself is modified: lignin is depolymerized and the free volume in the cell wall increased by component removal, potentially improving bonding by allowing more polymer interdiffusion and interaction at the surface.[48,49] The chemical difference between the top and bottom may also relate to the difference in the main component of hyphae at different locations (top and bottom), which could not be separated here.

Because the bonds always fail on the top side of the mycelium layer, the exact bond strength between the bottom surface of mycelium layer and veneer surface is not possible to be measured in the current experimental setup. It should be highlighted that, although the adhesion ability of the top surface is weaker than that of the bottom surface, it is still a competitive candidate for wood bonding. We tested commercial wood glue for comparison: the lap-shear strength was 1.72 (±0.54) MPa, which showed no significant difference ($p > 0.05$) from the lap-shear strength of the sample made with mycelium on degraded wood (Day 8) and slightly higher than that formed with mycelium on untreated wood. Moreover, after water soaking, the commercial wood glue-bonded samples completely fell apart, whereas although the mycelium adhesive also lost the majority of its strength (the lap-shear strength dropped to 0.27 ± 0.10 MPa), the two pieces of wood could still hold together. Thus, mycelium growth could be at the minimum a potentially efficient pretreatment method for producing all-natural biocomposites such as packaging materials, insulation board, particleboard, and fiberboard. Moreover, as the surface layer of mycelium is very easy to remove and apply to untreated wood, they could also be considered as a novel stand-alone adhesive.

The mycelium used in the current research is directly produced from harvest with no grinding, extraction, or combination with other cross-linkers. Multiple approaches could be followed to further improve its bonding strength and water resistance. For the wood pretreatment purpose, mixing the growing system continuously may stop the development of aerial hyphae, only biofilm hyphae would exist at the interfaces,[20] and the adhesion could be improved. For the stand-alone adhesive purposes, surface mycelium could be produced at a large-scale in bioreactors with more control of the nutrient supply and air flow.[50] As the mycelium composition and surface properties are highly influenced by the nutrient source, the attaching surface, and the growing environment,[22,23] it could be worthwhile to increase the active functional groups on the surface through controlling the substrate. Alternatively, very limited fungal species (36 according to Elsacker et. al[1]) have been investigated in mycelium-based composite production and they are restricted to the Basidiomycota phylum due to their ability to grow large mycelium networks. However, in our current work, we discovered that the density and thickness of the surface mycelium layer is not crucial in bonding after hot-pressing. In this case, more species of fungi could be investigated with the purpose of finding a more active and functional interface.

CONCLUSIONS

The colonization of white-rot fungi *Trametes versicolor* on yellow birch veneers provided promising bonding on wood. The adhesion strength achieved was higher than that potentially caused by the physical or chemical changes of the wood surface only. The best pretreatment time was found to be 8 days; at this time, the mycelium covered the entire surface with no apparent weight loss of wood and provided the best bonding performance. Our results showed that the surface mycelium layer could also be utilized as a stand-alone adhesive to bond untreated wood. The bottom surface of the mycelium was found to be denser, flatter, and more hydrophilic and provided a stronger bonding than that of the top surface. This work demonstrates the importance of surface mycelium interfaces in wood bonding and provides useful information for the development of biobased materials, such as fungal-pretreated lignocellulosic biocomposites and novel mycelium-based adhesives.

AUTHOR INFORMATION

Corresponding Author

Mehdi Tajvidi − *Laboratory of Renewable Nanomaterials, School of Forest Resources and Advanced Structures and Composites Center, University of Maine, Orono, Maine 04469-5755, United States;* orcid.org/0000-0002-3549-1220; Email: mehdi.tajvidi@maine.edu

Authors

Wenjing Sun − *Laboratory of Renewable Nanomaterials, School of Forest Resources and Advanced Structures and Composites Center, University of Maine, Orono, Maine 04469-5755, United States*

Caitlin Howell − *Department of Chemical and Biomedical Engineering and Graduate School of Biomedical Science and Engineering, University of Maine, Orono, Maine 04469-5755, United States*

Christopher G. Hunt − *USDA Forest Products Laboratory, Madison, Wisconsin 53726, United States;* orcid.org/0000-0002-4799-7085

Complete contact information is available at: https://pubs.acs.org/10.1021/acsami.0c18165

Author Contributions

The manuscript was written through contributions of all authors. All authors have given approval to the final version of the manuscript.

Notes

The authors declare no competing financial interest.

https://dx.doi.org/10.1021/acsami.0c18165
ACS Appl. Mater. Interfaces 2020, 12, 57431−57440

■ ACKNOWLEDGMENTS

This work was supported by the U.S. Department of Agriculture's Agricultural Research Service (USDA ARS Agreement No. 58-0204-003). The authors thank Ecovative Design LLC for providing the mycelium culture and Columbia Forest Products LLC for providing wood veneers.

■ ABBREVIATIONS

CSL, corn steep liquor; MEA, malt extract agar; SEM, scanning electron microscopy; ATR-FTIR, attenuated total reflectance-Fourier transform infrared spectroscopy; TG, the variation of the sample mass; DTG, the derivative weight loss

■ REFERENCES

(1) Elsacker, E.; Vandelook, S.; Van Wylick, A.; Ruytinx, J.; De Laet, L.; Peeters, E. A Comprehensive Framework for the Production of Mycelium-Based Lignocellulosic Composites. *Sci. Total Environ.* **2020**, *725*, 138431.

(2) Girometta, C.; Picco, A. M.; Baiguera, R. M.; Dondi, D.; Babbini, S.; Cartabia, M.; Pellegrini, M.; Savino, E. Physico-Mechanical and Thermodynamic Properties of Mycelium-Based Biocomposites: A Review. *Sustainability* **2019**, *11* (1), 281.

(3) Jones, M.; Mautner, A.; Luenco, S.; Bismarck, A.; John, S. Engineered Mycelium Composite Construction Materials from Fungal Biorefineries: A Critical Review. *Mater. Des.* **2020**, *187*, 108397.

(4) Sun, W.; Tajvidi, M.; Hunt, C. G.; McIntyre, G.; Gardner, D. J. Fully Bio-Based Hybrid Composites Made of Wood, Fungal Mycelium and Cellulose Nanofibrils. *Sci. Rep.* **2019**, *9* (1), 1−12.

(5) Appels, F. V.; Camere, S.; Montalti, M.; Karana, E.; Jansen, K. M.; Dijksterhuis, J.; Krijgsheld, P.; Wosten, H. A. J. M. Design, Fabrication Factors Influencing Mechanical, Moisture-and Water-Related Properties of Mycelium-Based Composites. *Mater. Des.* **2019**, *161*, 64−71.

(6) Liu, R.; Long, L.; Sheng, Y.; Xu, J.; Qiu, H.; Li, X.; Wang, Y.; Wu, H. Preparation of a Kind of Novel Sustainable Mycelium/Cotton Stalk Composites and Effects of Pressing Temperature on the Properties. *Ind. Crops Prod.* **2019**, *141*, 111732.

(7) Hemmila, V.; Adamopoulos, S.; Karlsson, O.; Kumar, A. Development of Sustainable Bio-Adhesives for Engineered Wood Panels - a Review. *RSC Adv.* **2017**, *7* (61), 38604−38630.

(8) Hubbe, M. A.; Pizzi, A.; Zhang, H.; Halis, R. Critical Links Governing Performance of Self-Binding and Natural Binders for Hot-Pressed Reconstituted Lignocellulosic Board without Added Formaldehyde: A Review. *BioResources* **2017**, *13* (1), 2049−2115.

(9) Tajuddin, M.; Ahmad, Z.; Ismail, H. A Review of Natural Fibers and Processing Operations for the Production of Binderless Boards. *BioResources* **2016**, *11* (2), 5600−5617.

(10) Ge, S.; Chen, X.; Li, D.; Liu, Z.; Ouyang, H.; Peng, W.; Zhang, Z. Hemicellulose Structural Changes During Steam Pretreatment and Biogradation of *Lentinus Edodes*. *Arabian J. Chem.* **2018**, *11* (6), 771−781.

(11) Xiao, L.-P.; Shi, Z.-J.; Bai, Y.-Y.; Wang, W.; Zhang, X.-M.; Sun, R.-C. Biodegradation of Lignocellulose by White-Rot Fungi: Structural Characterization of Water-Soluble Hemicelluloses. *Bio-Energy Res.* **2013**, *6* (4), 1154−1164.

(12) Cragg, S. M.; Beckham, G. T.; Bruce, N. C.; Bugg, T. D. H.; Distel, D. L.; Dupree, P.; Etxabe, A. G.; Goodell, B. S.; Jellison, J.; McGeehan, J. E.; McQueen-Mason, S. J.; Schnorr, K.; Walton, P. H.; Watts, J. E. M.; Zimmer, M. Lignocellulose Degradation Mechanisms across the Tree of Life. *Curr. Opin. Chem. Biol.* **2015**, *29*, 108−119.

(13) Sigoillot, J.-C.; Berrin, J.-G.; Bey, M.; Lesage-Meessen, L.; Levasseur, A.; Lomascolo, A.; Record, E.; Uzan-Boukhris, E. Chapter 8 - Fungal Strategies for Lignin Degradation. In *Advances in Botanical Research*; Jouanin, L., Lapierre, C., Eds.; Academic Press, 2012; Vol. *61*, pp 263−308.

(14) Pollegioni, L.; Tonin, F.; Rosini, E. Lignin-Degrading Enzymes. *FEBS J.* **2015**, *282* (7), 1190−1213.

(15) Janusz, G.; Pawlik, A.; Sulej, J.; Swiderska-Burek, U.; Jarosz-Wilkolazka, A.; Paszczynski, A. Lignin Degradation: Microorganisms, Enzymes Involved, Genomes Analysis and Evolution. *FEMS Microbiol. Rev.* **2017**, *41* (6), 941−962.

(16) Felby, C.; Nielsen, B.; Olesen, P.; Skibsted, L. Identification and Quantification of Radical Reaction Intermediates by Electron Spin Resonance Spectrometry of Laccase-Catalyzed Oxidation of Wood Fibers from Beech (Fagus Sylvatica). *Appl. Microbiol. Biotechnol.* **1997**, *48* (4), 459−464.

(17) Alvarez, C.; Rojano, B.; Almaza, O.; Rojas, O. J.; Ganan, P. Self-Bonding Boards from Plantain Fiber Bundles after Enzymatic Treatment: Adhesion Improvement of Lignocellulosic Products by Enzymatic Pre-Treatment. *J. Polym. Environ.* **2011**, *19* (1), 182−188.

(18) Wu, C.; Zhou, S.; Li, R.; Wang, D.; Zhao, C. Reactivity Improvement of Bamboo Dissolving Pulp by Xylanase Modification. *BioResources* **2015**, *10* (3), 4970−4977.

(19) Kharazipour, A.; Bergmann, K.; Nonninger, K.; Huttermann, A. Properties of Fibre Boards Obtained by Activation of the Middle Lamella Lignin of Wood Fibres with Peroxidase and H_2o_2 before Conventional Pressing. *J. Adhes. Sci. Technol.* **1998**, *12* (10), 1045−1053.

(20) Sugai-Guerios, M. H.; Balmant, W.; Furigo, A.; Krieger, N.; Mitchell, D. A. Modeling the Growth of Filamentous Fungi at the Particle Scale in Solid-State Fermentation Systems. In *Filaments in Bioprocesses*; Krull, R., Bley, T., Eds.; Springer International Publishing: Cham, 2015; pp 171−221.

(21) Rahardjo, Y. S. P.; Tramper, J.; Rinzema, A. Modeling Conversion and Transport Phenomena in Solid-State Fermentation: A Review and Perspectives. *Biotechnol. Adv.* **2006**, *24* (2), 161−179.

(22) Haneef, M.; Ceseracciu, L.; Canale, C.; Bayer, I. S.; Heredia-Guerrero, J. A.; Athanassiou, A. Advanced Materials from Fungal Mycelium: Fabrication and Tuning of Physical Properties. *Sci. Rep.* **2017**, *7* (1), 41292.

(23) Antinori, M. E.; Ceseracciu, L.; Mancini, G.; Heredia-Guerrero, J. A.; Athanassiou, A. Fine-Tuning of Physicochemical Properties and Growth Dynamics of Mycelium-Based Materials. *ACS Appl. Bio Mater.* **2020**, *3* (2), 1044−1051.

(24) de Almeida, F. P.; Freire, D. M. G.; Lins, U.; Gutarra, M. L. E. Surface Imaging of the Filamentous Fungus Penicillium Simplicissimum Growing in a Solid-State Fermentation System. *Micron* **2017**, *99*, 19−25.

(25) Steudler, S.; Bley, T. Better One-Eyed Than Blind—Challenges and Opportunities of Biomass Measurement During Solid-State Fermentation of Basidiomycetes. In *Filaments in Bioprocesses*; Krull, R., Bley, T., Eds.; Springer International Publishing: Cham, 2015; pp 223−252.

(26) Gow, N. A. R.; Latge, J. P.; Munro, C. A. The Fungal Cell Wall: Structure, Biosynthesis, and Function. *Microbiol. Spectr.* **2017**, *5* (3), 25.

(27) Cheng, H.; He, Z. Wood Adhesives Containing Proteins and Carbohydrates. *Bio-Based Wood Adhesives: Preparation, Characterization*; CRC Press, 2017; pp 140−155.

(28) Fackler, K.; Schmutzer, M.; Manoch, L.; Schwanninger, M.; Hinterstoisser, B.; Ters, T.; Messner, K.; Gradinger, C. Evaluation of the Selectivity of White Rot Isolates Using near Infrared Spectroscopic Techniques. *Enzyme Microb. Technol.* **2007**, *41* (6−7), 881−887.

(29) Fackler, K.; Schwanninger, M.; Gradinger, C.; Hinterstoisser, B.; Messner, K. J. F. m. l. Qualitative and Quantitative Changes of Beech Wood Degraded by Wood-Rotting Basidiomycetes Monitored by Fourier Transform Infrared Spectroscopic Methods and Multivariate Data Analysis. *FEMS Microbiol. Lett.* **2007**, *271* (2), 162−169.

(30) Schneider, C. A.; Rasband, W. S.; Eliceiri, K. W. NIH Image to ImageJ: 25 Years of Image Analysis. *Nat. Methods* **2012**, *9* (7), 671−675.

(31) Appels, F. V. W.; Dijksterhuis, J.; Lukasiewicz, C. E.; Jansen, K. M. B.; Wosten, H. A. B.; Krijgsheld, P. Hydrophobin Gene Deletion

and Environmental Growth Conditions Impact Mechanical Properties of Mycelium by Affecting the Density of the Material. *Sci. Rep.* **2018**, *8* (1), 4703.
(32) Sammer, D.; Krause, K.; Gube, M.; Wagner, K.; Kothe, E. Hydrophobins in the Life Cycle of the Ectomycorrhizal Basidiomycete *Tricholoma Vaccinum*. *PLoS One* **2016**, *11* (12), e0167773.
(33) Landry, V.; Blanchet, P. J. F. P. J. Surface Preparation of Wood for Application of Waterborne. *Coatings.* **2012**, *62* (1), 39−45.
(34) Hakkou, M.; Petrissans, M.; Zoulalian, A.; Gerardin, P. Investigation of Wood Wettability Changes During Heat Treatment on the Basis of Chemical Analysis. *Polym. Degrad. Stab.* **2005**, *89* (1), 1−5.
(35) Grønli, M. G.; Varhegyi, G.; Di Blasi, C. Thermogravimetric Analysis and Devolatilization Kinetics of Wood. *Ind. Eng. Chem. Res.* **2002**, *41* (17), 4201−4208.
(36) Zhai, M.; Guo, L.; Zhang, Y.; Dong, P.; Qi, G.; Huang, Y. Kinetic Parameters of Biomass Pyrolysis by TGA. *BioResources* **2016**, *11* (4), 8548−8557.
(37) Hostikka, S.; Matala, A. Pyrolysis Model for Predicting the Heat Release Rate of Birch Wood. *Combust. Sci. Technol.* **2017**, *189* (8), 1373−1393.
(38) Wu, J.; Chen, C.; Zhang, H.; Xia, L.; Huang, Y.; Huang, H.; Wang, Y.; Qian, D.; Wang, J.; Wang, X.; Zhang, T. Eco-Friendly Fiberboard Production without Binder Using Poplar Wood Shavings Bio-Pretreated by White Rot Fungi Coriolus Versicolor. *Constr Build Mater.* **2020**, *236*, 117620.
(39) Jones, M. P.; Lawrie, A. C.; Huynh, T. T.; Morrison, P. D.; Mautner, A.; Bismarck, A.; John, S. Agricultural by-Product Suitability for the Production of Chitinous Composites and Nanofibers Utilising *Trametes Versicolor* and *Polyporus Brumalis* Mycelial Growth. *Process Biochem.* **2019**, *80*, 95−102.
(40) Naumann, A. A Novel Procedure for Strain Classification of Fungal Mycelium by Cluster and Artificial Neural Network Analysis of Fourier Transform Infrared (FTIR) Spectra. *Analyst* **2009**, *134* (6), 1215−1223.
(41) Lecellier, A.; Mounier, J.; Gaydou, V.; Castrec, L.; Barbier, G.; Ablain, W.; Manfait, M.; Toubas, D.; Sockalingum, G. D. Differentiation and Identification of Filamentous Fungi by High-Throughput FTIR Spectroscopic Analysis of Mycelia. *Int. J. Food Microbiol.* **2014**, *168*−*169*, 32−41.
(42) Nooshkam, M.; Madadlou, A. Maillard Conjugation of Lactulose with Potentially Bioactive Peptides. *Food Chem.* **2016**, *192*, 831−836.
(43) Girometta, C.; Dondi, D.; Baiguera, R. M.; Bracco, F.; Branciforti, D. S.; Buratti, S.; Lazzaroni, S.; Savino, E. Characterization of Mycelia from Wood-Decay Species by TGA and IR Spectroscopy. *Cellulose* **2020**, *27* (11), 6133−6148.
(44) Duvnjak, D.; Pantic, M.; Pavlovic, V.; Nedovic, V.; Levic, S.; Matijasevic, D.; Sknepnek, A.; Niksic, M. Advances in Batch Culture Fermented Coriolus Versicolor Medicinal Mushroom for the Production of Antibacterial Compounds. *Innovative Food Sci. Emerging Technol.* **2016**, *34*, 1−8.
(45) Xiao, X.; Hou, Y.; Du, J.; Liu, Y.; Liu, Y.; Dong, L.; Liang, Q.; Wang, Y.; Bai, G.; Luo, G. Determination of Main Categories of Components in Corn Steep Liquor by near-Infrared Spectroscopy and Partial Least-Squares Regression. *J. Agric. Food Chem.* **2012**, *60* (32), 7830−7835.
(46) Hofer, A.; Hauer, S.; Kroll, P.; Fricke, J.; Herwig, C. In-Depth Characterization of the Raw Material Corn Steep Liquor and Its Bioavailability in Bioprocesses of *Penicillium Chrysogenum*. *Process Biochem.* **2018**, *70*, 20−28.
(47) Zabel, R. A.; Morrell, J. J. Chapter Five - Fungal Metabolism in Relation to Wood Decay. In *Wood Microbiology*, Second Ed.; Zabel, R. A., Morrell, J. J., Eds.; Academic Press: San Diego, 2020; pp 129−148.
(48) Herrera, R.; Erdocia, X.; Labidi, J.; Llano-Ponte, R. Chemical Analysis of Industrial-Scale Hydrothermal Wood Degraded by Wood-Rotting Basidiomycetes and Its Action Mechanisms. *Polym. Degrad. Stab.* **2015**, *117*, 37−45.
(49) Bari, E.; Taghiyari, H. R.; Naji, H. R.; Schmidt, O.; Ohno, K. M.; Clausen, C. A.; Bakar, E. S. Assessing the Destructive Behaviors of Two White-Rot Fungi on Beech Wood. *Int. Biodeterior. Biodegrad.* **2016**, *114*, 129−140.
(50) Bajoul Kakahi, F.; Ly, S.; Tarayre, C.; Deschaume, O.; Bartic, C.; Wagner, P.; Compere, P.; Derdelinckx, G.; Blecker, C.; Delvigne, F. Modulation of Fungal Biofilm Physiology and Secondary Product Formation Based on Physico-Chemical Surface Properties. *Bioprocess Biosyst. Eng.* **2019**, *42* (12), 1935−1946.

https://dx.doi.org/10.1021/acsami.0c18165
ACS Appl. Mater. Interfaces 2020, 12, 57431−57440